GEM-TN-93-285

ALTERNATIVE TRIGGER SCHEME FOR THE GEM

L. Barabash, V. Frolov, V. Kalunnikov, K. Kuznetsov, A. Popov, S. Selunin, Yu. Yatsunenko
Joint Institute for Nuclear Research, Dubna, Russia

January 18, 1993

Abstract:

We try to show an alternative trigger scheme of GEM. Slow drift detector signals are used for the generation of timed trigger signals in this scheme. We show possible realizations of this idea in the GEM muon system.

INTRODUCTION

The use of a large number of drift detectors usually requires an external trigger system. But with a large drift detector system, the problem of creating of an external trigger system arises.

The main idea of generation of fast trigger signals was posed in ref. [1]. In this brief report we describe the results of our investigations of the separation of different solutions and show a possible muon trigger system for the PDT option.

The solutions used to calculate the time interval from the last pulse in a triplet of detector layers to the time of generation of a trigger signal are the following:

Solution 1. $X_1 = T/2 - (t1/2 + t2/4)$

Solution 2. $X_2 = t2/2 - t1$

Solution 3. $X_3 = T - (t1 - t2/2)$

Solution 4. $X_4 = t2/2$

where T is the total drift time,

$$t1 = |T_2 - \max T_{1,3}|$$

$$t2 = |T_1 - T_3|$$

and the condition when we lose the resolution of left-right ambiguity is

$$t2/2 - t1 = 0 \quad \text{when } t1 \text{ and } t2 \neq 0.$$

When this condition is true, a trigger signal cannot be generated. This is the feature of any drift detector.

1.0 ONE TRACK TRIGGER PROTOTYPE

One of the main problems in the generation of fast trigger signals for the suggested scheme is the rejection of ghost decisions and the choice of right triggers. The conditions of the straight line and angle of registered tracks can be used for these goals. These conditions were investigated in detail in ref. [2]. We would like to have a fast decision prototype without complex mathematical operations, and so when designing we chose the following rejection conditions:

- We used the complex OR. It allows solution 3, and the condition, when we lose the resolution of left-right ambiguity (t1=t2/2), to be separated from solutions 1, 2 and 4 using the hardware decision.
- We excluded solution 2. In this case the prototype covers an angular range of up to 12 degrees and provides the trigger from 10 GeV/c muons for a 32-sector muon system.
- We used simple conditions for the separation of solutions 1 and 4:

$$S1 \equiv (t1A = t1B) \cap (t2A \neq t2B)$$

This condition chooses the 1A-4B and 4A-1B pairs of solutions in triplets A and B. We don't separate these pairs because a wrong solution gives a delayed ghost pulse. As the investigations of the rejection of false triggers show, condition S1 is not enough for a reliable isolation of these pairs of solutions. We are forced to turn on an additional condition:

$$S2 \equiv (X1=X4) \text{ or} \equiv (T = t\,1A + t2A/2 + t2B), (T = t1B + t2B/2 + t2A)$$

To separate the 1A-1B pair of solutions, we used the condition:

$$S3 \equiv (t2A = t2B)$$

The events with a loss of left-right ambiguity are separated using the following conditions:

$$S4 \equiv (t1A = t2A/2) \cup (t1B = t2B/2)$$

The use of condition S4 allows one to prohibit the generation of trigger and to mark these events.

1.1 Computing Part of the Prototype

After excluding solution 2, we should realize the calculation of "x" using solutions 1, 3 and 4 which can be written in the following form:

Solution 1	$X_1 = X3/2$
Solution 3	$X_3 = T - (t1+t2/2)$
Solution 4	$X_4 = t2/2$

Thus, the calculation should be only performed for solution 3 which can be realized using fast programmable matrix memory chips with internal delay less than 8 nsec.

1.2. Description of a Logical Scheme of the Prototype

A logical scheme of the prototype (see fig. 1) includes the following parts:

- Control Scheme

  This part provides the measurement of time intervals between pulses from the sensitive wires of the superlayer and the generation of a necessary time sequence of control pulses for the other parts of the prototype.

- Condition Generation Part

  This part provides the generation of conditions for separation of solutions by comparing the measured values of t1A, t2A and t1B, t2B.

- Computing part

- Time Correction part

1.3 Results of Separation of Different Solutions with Cosmic Rays

Cosmic ray tracks were used to investigate different separation conditions (the scheme was the same as part of the PDR superlayer). Ar + 9% CO2 was used as a gas mixture [3].

The drift coordinates of the tracks were used for the separation of different solution branches (1A-1B, 1A-4B, 4A-1B). This step allows the precision of track registration to be estimated.

As seen from the scheme of "complex OR", the main problem is to separate the pair of solutions 1A-1B from the 1A-4B and 4A-1B pairs. The pair of 1A-1B should be isolated from the others because solutions 4A and 4B give ghost triggers when the 1A-1B pair works. Figure 2 shows the distribution of t2A-t2B for the tracks identified for the 1A-1B branch.

The rejection ability was checked using all tracks without any cuts. The tracks had to satisfy one condition only: all four tubes gave pulses. We obtained the following results:

Conditions	Pair of sol.	Level of a ghost signal
with no cuts	1A-1B	17%
	1A-4B, 4A-1B	more than 50%
t2A = t2B (± 50ns)	1A-1B	(3.9 - 4.3)%
t2A ≠ t2B, t1A = t1B (10 ns) X1 = X4 (50 ns)	1A-4B, 4A-1B	Sol. 1 (4.3 - 4.6)% Sol. 4 (1 - 1.5)%
Precision of detectors near 0.5mm	1A-1B	2.7%
	1A-4B, 4A-1B	< 0.5%

We show a distribution of all tracks having passed through the 1A-1B branch with no cuts (see fig. 3) and the level of ghost triggers in this case. Figure 4 shows the power ability of condition t2A-t2B. The level of ghost signals is rejected from 17% to 4%.

A good precision of detectors is very important because this decreases overlap zones of the rejection conditions.

1.4 Systematic Errors

The main systematic error is nonlinearity of the x=f(t) detector characteristic. The values of t1 can be used to correct this error. Figure 5 shows the correction ability of these parameters.

The following systematic error determined by measuring the track radius of round drift tubes can corrected using the values of t2. The set of solutions for the drift tube triplet was written on condition that the distances between the layers of the detectors are equal. It is not true when the track has an angle relative to the superlayer plane, and should be corrected.

1.5 Statistical Errors

The statistical errors of different solutions are the following:

$$\sigma_1 = \sigma_i \sqrt{5/8}$$

$$\sigma_3 = \sigma_i \sqrt{5/2}$$

$$\sigma_4 = \frac{\sigma_i}{\sqrt{2}}$$

where σ_i is the precision of the detectors.

Taking into account the error in the fast calculation starting time (we should include additional σ_i), the errors of trigger from different solutions look like:

$$\sigma_{tr1} = \sigma_i \sqrt{13/8}$$

$$\sigma_{tr3} = \sigma_i \sqrt{7/2}$$

$$\sigma_{tr4} = \sigma_i \sqrt{3/2}$$

As it follows from these equations, solution 3 gives a maximum error.

We can estimate the angular precision for a single triplet. If the precision of the detectors equals 0.1mm, the error in measuring muon angle is 13 mrad for solution 3 and 5.3 mrad for solutions 1 and 4. This allows one to have a good selectivity in muons P_t. We believe that it is a very important advantage of the suggested trigger system.

2.0 Architecture of the Trigger Muon System

At present the scheme of placement of the GEM muon detectors contains 16 sectors (GEM Baseline I), and a 32-sector scheme is being discussed [4]. In this case the requirements for trigger blocks are somewhat less than for the 16-sector scheme, and it is necessary to provide the acceptance in muon angle up to 11 degrees.

The second way of angular range reduction is the orientation of detectors by projection to the I. P. as suggested for the SDC muon system.

The trigger muon system should contain radial-symmetrical towers with phi-angle overlaps. The overlaps should provide effective registration of both sign muons with a momentum of no less than 10 GeV/c. The dimensions of the overlaps for this condition are (see fig. 6):

SL3	532 mm
SL2	380 mm
SL1	235 mm

and the minimum size of a single trigger block of the detectors should be two times larger.

2.1 High Rate Estimations and Possible Dimension of Detector Trigger Blocks

The results of calculation of an admissible rate of particles which defines the sizes of trigger blocks by phi are given in fig. 7a and b. These estimations were done for the dimension of the trigger blocks equal to the size of the overlaps (fig 7a) and for the trigger blocks which are two times less than the overlaps (SL3-266 mm, SL2 - 190mm, SL3 - 114mm, fig. 7b). Lines 1 and 2 are for one-track trigger electronics, lines 1' and 2' for two-track trigger electronics. Line 1 and 1' show the high rate when the level of inefficiency of registration is less than 5% and lines 2 and 2' for an inefficiency level of 10%.

In this case the numbers of trigger channels and detector trigger blocks are:

SL1	1536
SL2	2304
SL3	1536
Total number of channels	5376

A possible use of additional stereo superlayers for the measurement of second track coordinates can increase the number of channels in SL3 up to 3072 and in SL2 up to 3456. The total number of channels in the trigger system will contain 8064.

2.2 Multi Track Trigger Scheme

Another approach can be used for the solution of this problem. The function of start time delay F(Tst) can be used as a track criterion. This function equal to (N-1) (N-2) for track difference coordinates (N is the number of layers in the superlayer) is less for ghost difference coordinates. The maxima of this function show tracks with different times of flight through the superlayer. A more detailed description of this approach will be presented in ref. [5]. It seems that it looked quite complex for electronics realization now, but it should be studied very attentively.

At the present time we are going to continue efforts in realization of the simple scheme described in this paper and try to develop it to the two track scheme.

2.3 Measurement of the Second Coordinate of Muon Tracks

It seems it is not necessary to create a separate system for measuring the second coordinate of muons, and a better way is to use more completely the system for precise measurements of phi-coordinates. In connection with this we would like to come back to the discussion of measurement of the second coordinate using the charge division method.

In addition, we would like to pay attention ref. [4] in which it was suggested to use additional superlayers with a small stereo angle. This provides the measurement of the second coordinate with a (10-20)mm precision and can be used for increasing the efficiency of the trigger system. We discuss these problems in Appendix 1 in more detail.

APPENDIX 1

Comments to the PDT Readout System

A large number of electronics channels of the PDT readout system makes us search for another version of readout system. One of these versions is the encoding of electronics channels.

Encoding schemes give a sufficient reduction in the number of channels, but they have a limited application which can be explained by the errors in increasing the rate of particles. The main reason of these errors is the absence of criteria for matching a responded channel. Besides, the use of encoding requires quite a tight packing of detectors.

Another situation arises when we have a system of tight packing of drift tubes as in the GEM muon system. The encoding scheme becomes very simple. And the main things is that we have a match criterion. This is drift time.

Figure 8 shows a possible version of connection of drift tubes using the encoding matrix scheme. The number of channels excluding amplifiers and shapers, does not change and remains equal to the number of drift tubes:

$$n = L + M * N$$

as shown in figure 8. N is the number of groups by the φ coordinate, the L number of connected tubes by the R-coordinate and M the number of detector layers in the matrix.

For example, the PDT detector block of SL2 has 256 drift tubes. If we connect four tubes by the radius using fast OR, L=32. The number of groups by the phi-coordinate is equal to 6 (this is the requirement of the trigger scheme) and the number of connected layers M is 4. In this case we obtain the total number of channels equal to 112 instead of 256 and a rejection factor of 2.3. The growth of the number of connected layers allows this ratio to be increased.

In this case the main problem is the initiation of ghost pairs of tubes (as shown in fig.8). This effect depends on the resolution of time coordinate measurements. Figure 9 depicts the level of ghost pairs as a function of encoding level by the number of connected layers (left scale) and the ratio of the numbers of channels for a usual scheme to the scheme with encoding (right scale). The line P2 shows a probability of one ghost pair and line P3 for two ghost pairs. It is clear that the use of encoding allows a noticeable ratio to be realized. The time resolution equal to 1.5ns was taken in these estimations. These results can be checked with the PDT data obtained during TTR tests.

Estimate for the total number of electronics channels with encoding for M = 4.

Number of layers		Number of groups	Number of φ groups per sector	Total number of φ *gr.*	Number of channels
		(N)		(L)	
SL1	8	768×2	20×2	5184	11328
SL2	8	1152×2	32×2	12288	21504
SL3	4	1536	44	11264	17408
					50240
Total Number of PDT readout channels					

We would like to demonstrate the total number of PDT muon system channels for the following conditions:

SL1	3 superlayers, diameter of tubes	25mm, M=6
SL2	3 superlayers, diameter of tubes	38mm, M=6
SL3	2 superlayers, diameter of tubes	38mm, M=8

	(N)	(L)	
SL1	768×2	5184	14400
SL2	1152×2	12288	26112
SL3	1536	11264	23552
Total number of PDT readout channels			64064

In the frame of such a muon system we can provide the measurement of the second coordinate using three 4-layer superlayers with an additional measurement of the second coordinate by the charge division method. It is very important to have tracking match for such a system, and this step provides this requirement.

References:

1 L. Barabash, C. Bromberg, Yu. Fisyak et al., Generation of a Precisely Timed Muon Trigger Using Signals from the GEM Drift Tubes, GEM TN 92-161.

2 A. T. M. Wang, Triplet Coincidence in Drift Tubes for a Level 1 Muon Trigger, SDC-92- 378.

3 L. Barabash, V. Frolov, V. Kalinnikov et al., Investigation of Trigger Generation Using Signal from the Drift Tubes (to be published in JNIR Communication)

4 C. Bromberg, A Muon Tracking System for the GEM Detector Using Pressurized Drift Tubes, GEM TN-92-205.

5 Yu. Yatsunenko, Multi-track Trigger (to be published in JINR Communications).

Figure Captions:

Figure 1. Logical scheme of the trigger block prototype

Figure 2. Distribution of (t2S-t2B) for cosmic particles.

Figure 3. Distribution of calculated trigger pulses with no cuts for 1A-1B pair of solutions.

Figure 4. Rejection of the ghost trigger level using t2A=t2B condition

Figure 5. Correction ability of t1.

Figure 6. The sizes of overlaps for 10 GeV/c muons.

Figure 7. and Admissible rate of particles for one-track trigger and two-track trigger electronics different levels of inefficiency (lines 1, 1'-5%, 2.2'-10%).

Figure 8. Encoding scheme for 8-layer superlayer and possible ghost pairs of tubes.

Figure 9. A probability of initiation of a one ghost tube pair (P2) and two ghost pair (P3, left scale). A ratio of the number of channels for a usual sheme to the scheme with encoding (left scale).

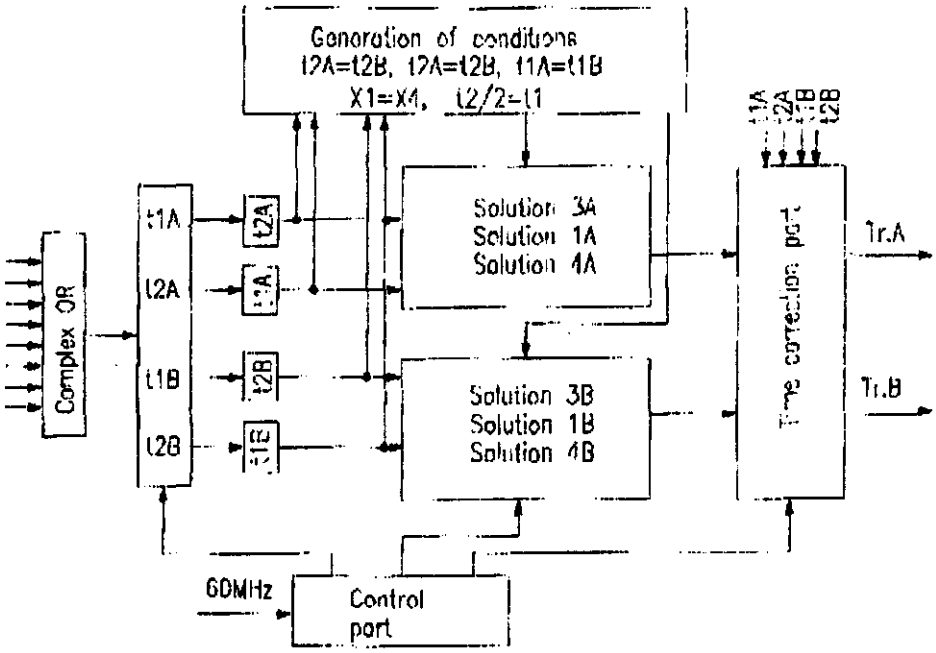
Generation of conditions
t2A=t2B, t2A=t2B, t1A=t1B
X1=X4, t2/2=t1
Complex OR
t1A
t2A
t1B
t2B
t2A
t1A
t2B
t1B
Solution 3A
Solution 1A
Solution 4A
Solution 3B
Solution 1B
Solution 4B
t1A
t2A
t1B
t2B
Tr.A
Tr.B
60MHz
Control
port

Fig. 1.

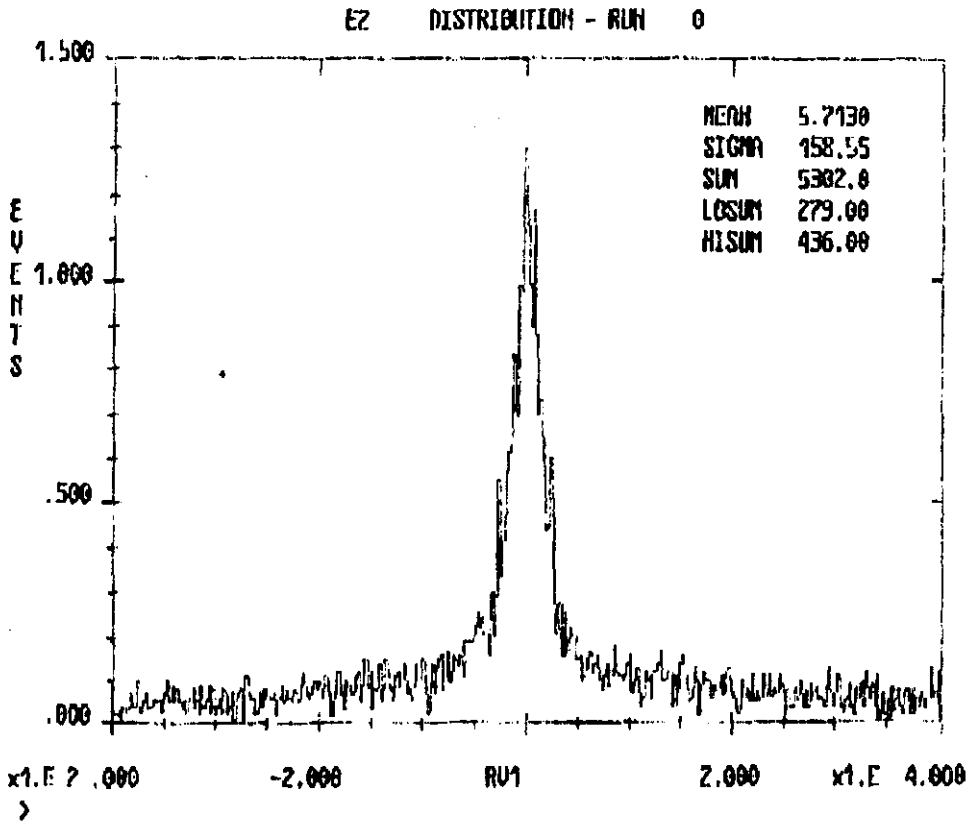
E2 DISTRIBUTION - RUN 0
1.500
1.000
.500
.000
EVENTS
MEAN 5.7130
SIGMA 158.55
SUM 5302.0
LOSUM 279.00
HISUM 436.00
x1.E 2 .000
-2.000
RU1
2.000
x1.E 4.000

Fig. 2.

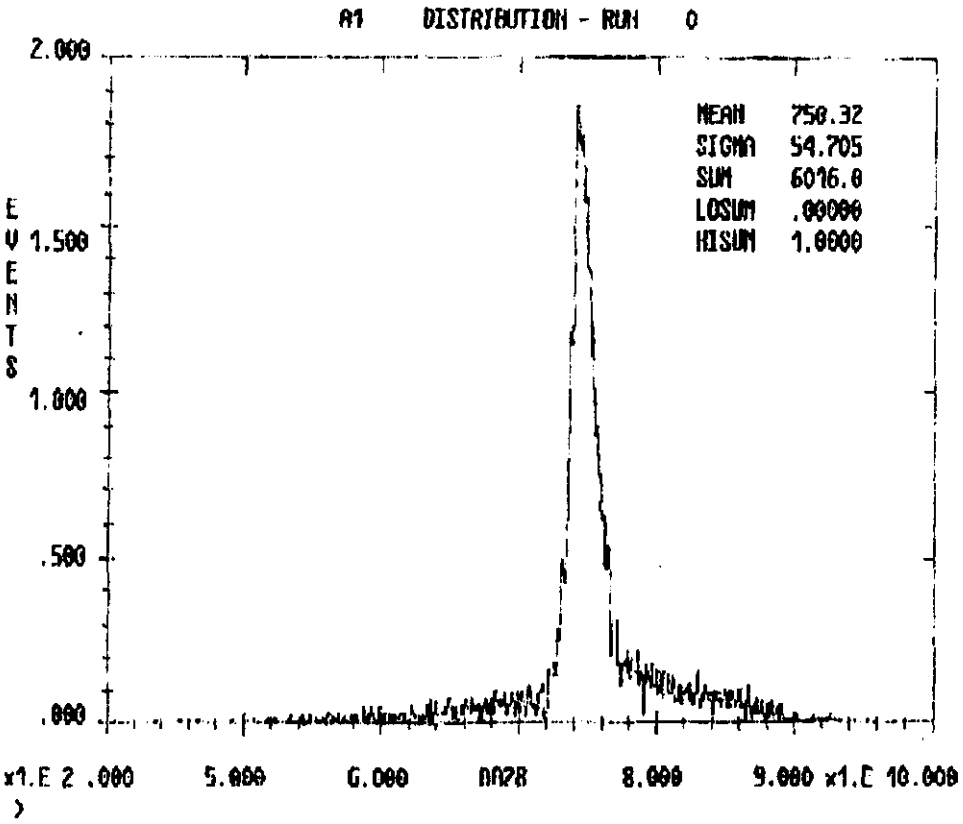
A1 DISTRIBUTION - RUN 0
MEAN 750.32
SIGMA 54.705
SUM 6016.0
LOSUM .00000
HISUM 1.0000
EVENTS
2.000
1.500
1.000
.500
.000
x1.E 2 .000
5.000
6.000
8.000
9.000 x1.E 10.000

Fig. 3.

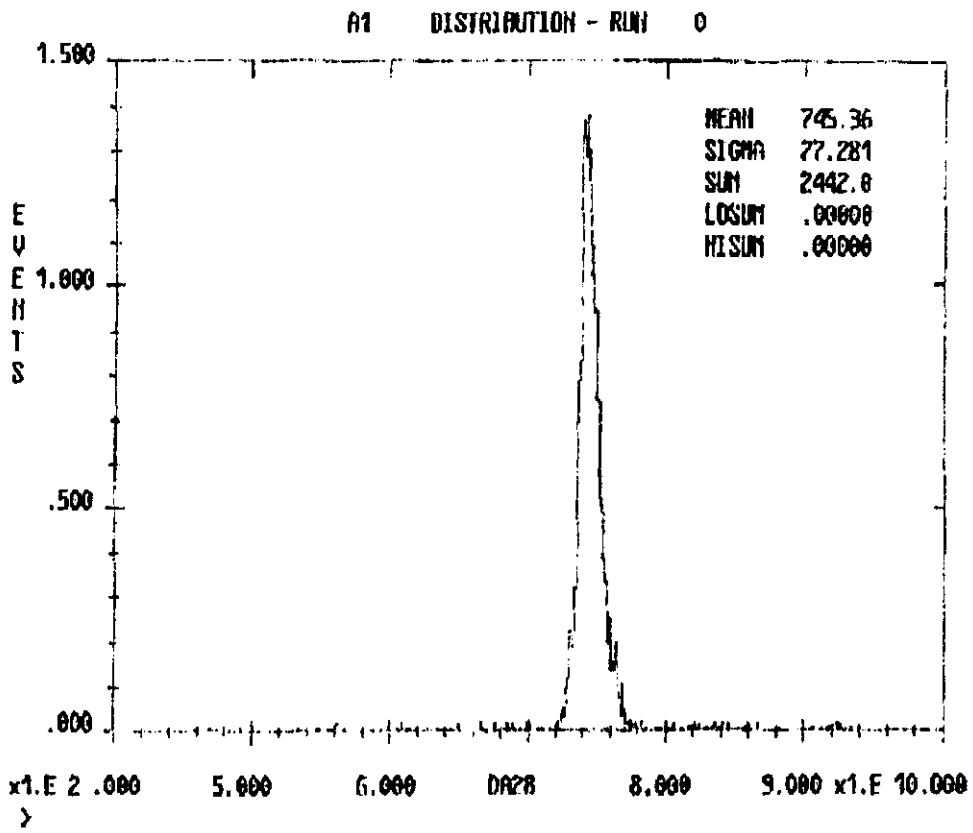
A1 DISTRIBUTION - RUN 0
1.500
1.000
.500
.000
EVENTS
MEAN 745.36
SIGMA 77.281
SUM 2442.0
LOSUM .00000
HISUM .00000
x1.E 2 .000
5.000
6.000
DA28
8.000
9.000 x1.E 10.000

Fig. 4.

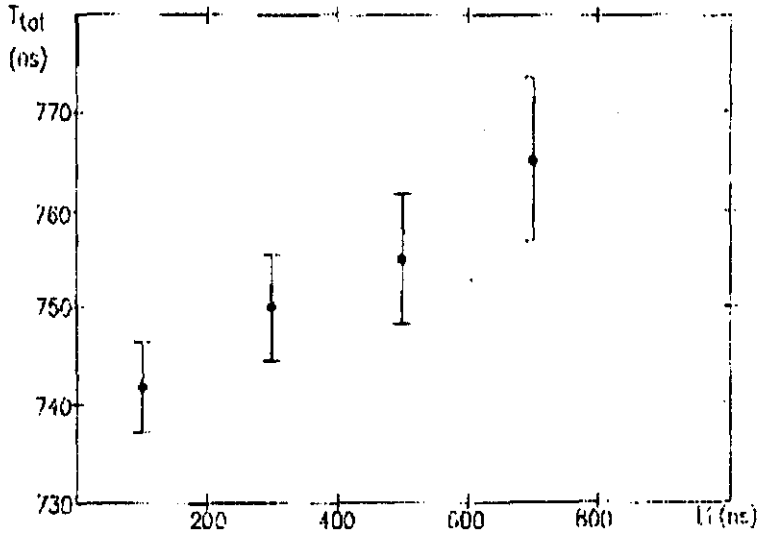

Fig. 5.

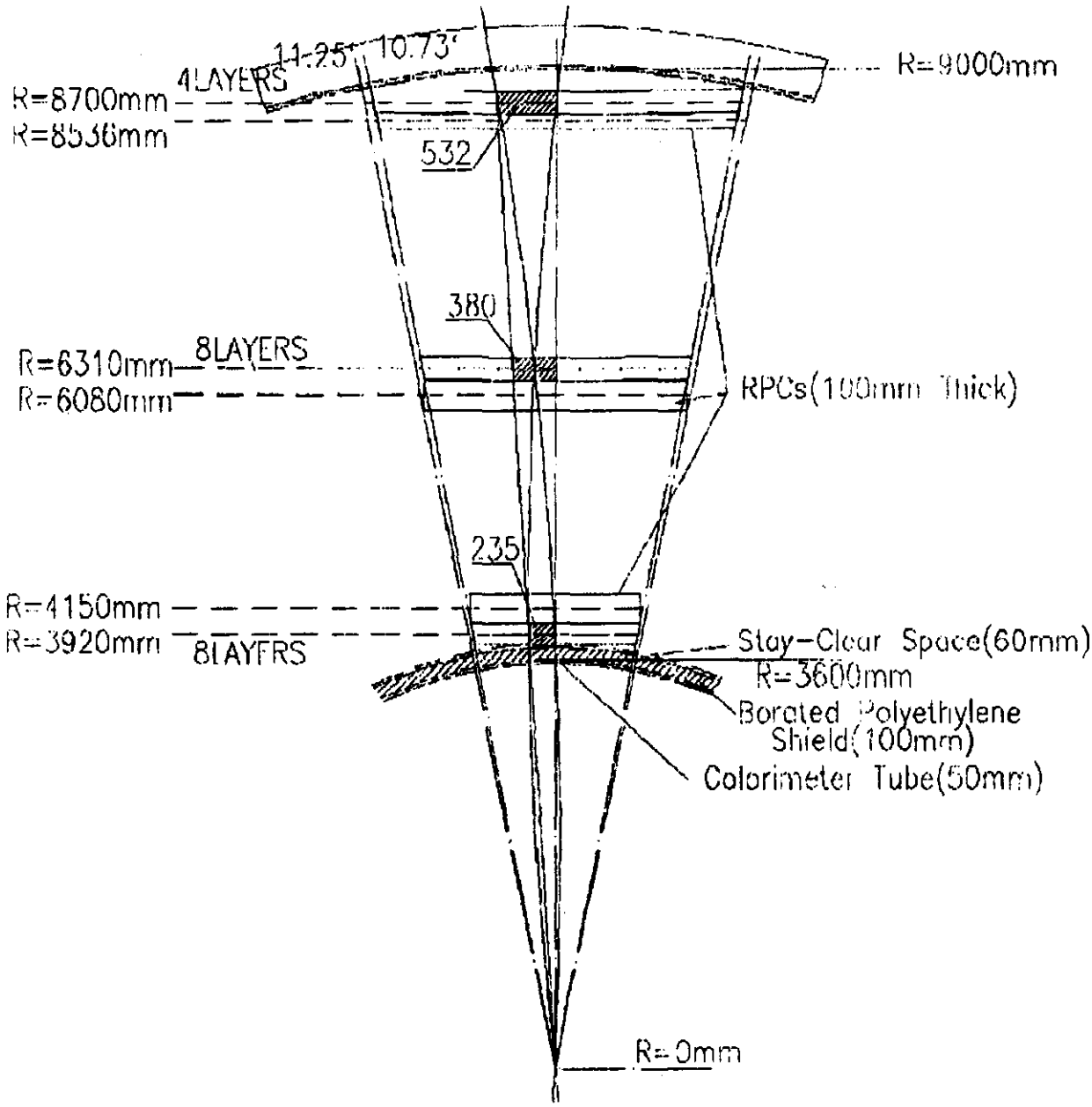
11.25°
10.73°
R=9000mm
R=8700mm
4LAYERS
R=8536mm
532
380
R=6310mm
8LAYERS
R=6080mm
RPCs(100mm Thick)
235
R=4150mm
R=3920mm
8LAYERS
Stay-Clear Space(60mm)
R=3600mm
Borated Polyethylene
Shield(100mm)
Colorimeter Tube(50mm)
R=0mm

Fig. 6.

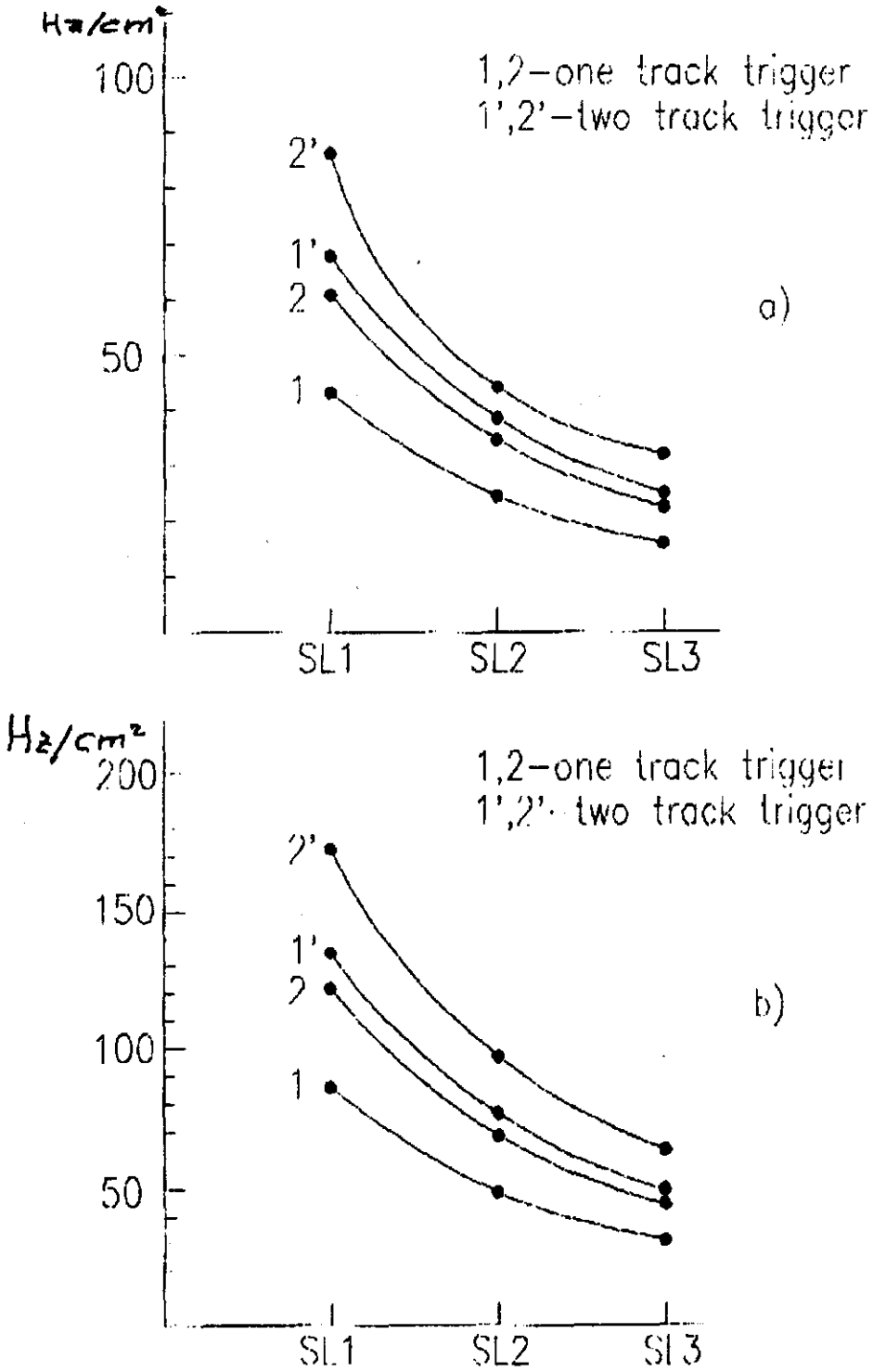
Hz/cm²
100
50
1,2–one track trigger
1',2'–two track trigger
2'
1'
2
1
a)
SL1
SL2
SL3
Hz/cm²
200
150
100
50
1,2–one track trigger
1',2'– two track trigger
2'
1'
2
1
b)
SL1
SL2
SL3

Fig. 7.

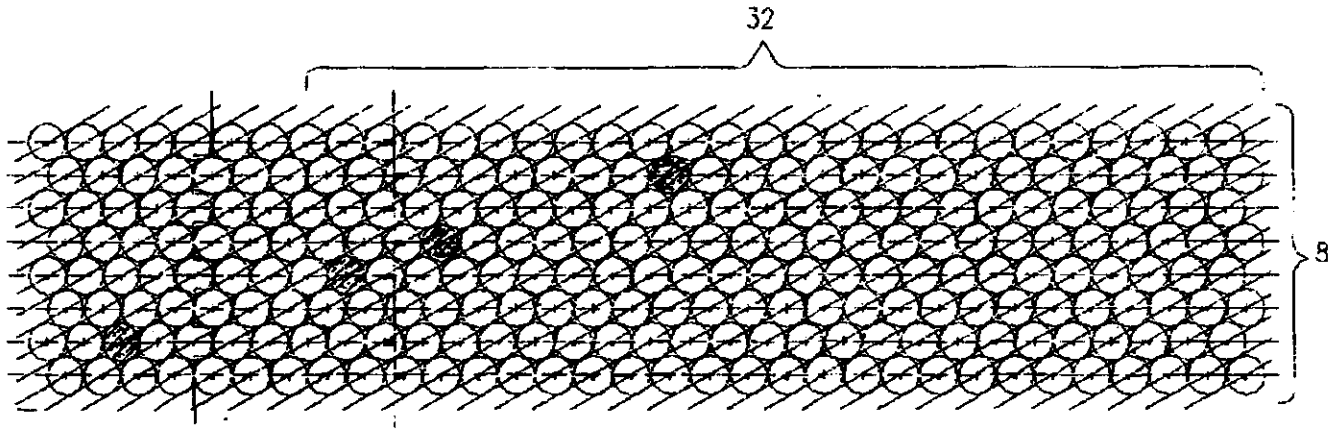

Fig. 8.

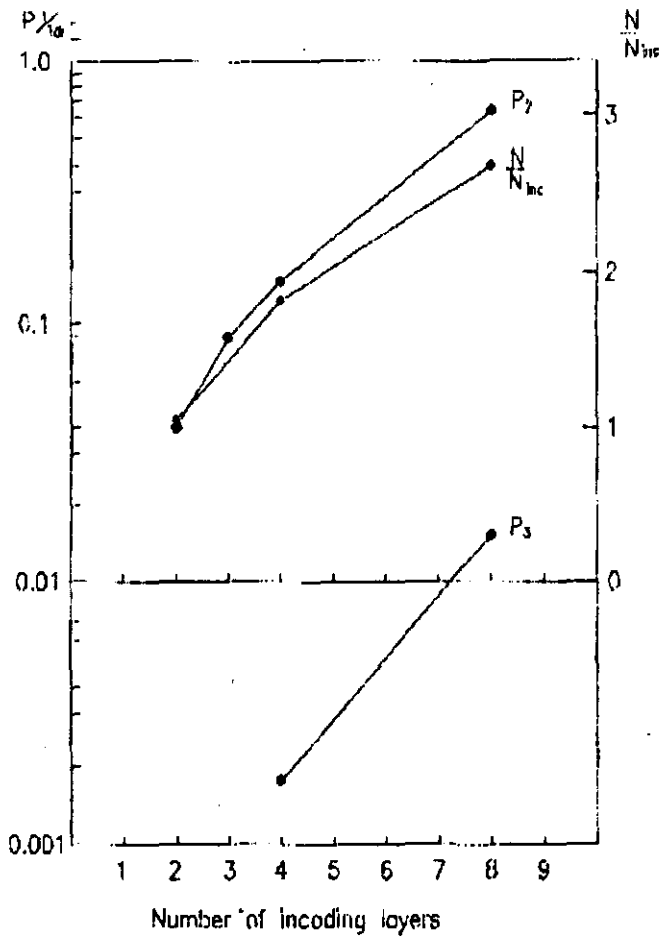

P/10
N/N_inc
1.0
0.1
0.01
0.001
3
2
1
0
P2
N/N_inc
P3
1 2 3 4 5 6 7 8 9
Number of incoding layers

Fig. 9.